BIOCHEMISTRY
including biophysical chemistry & molecular biology
Article

Biochemistry **2010,** *49,* 7033–7039 7033
DOI: 10.1021/bi100749p

Functional Role of Thr-312 and Thr-315 in the Proton-Transfer Pathway in ba_3 Cytochrome *c* Oxidase from *Thermus thermophilus*[†]

Irina Smirnova,[‡,⊥] Joachim Reimann,[‡] Christoph von Ballmoos,[‡] Hsin-Yang Chang,[§] Robert B. Gennis,[§] James A. Fee,[∥] Peter Brzezinski,[‡] and Pia Ädelroth*[,‡]

[‡]*Department of Biochemistry and Biophysics, The Arrhenius Laboratories for Natural Sciences, Stockholm University, SE-106 91 Stockholm, Sweden,* [§]*Department of Biochemistry, University of Illinois, Urbana, Illinois 61801, and* [∥]*Department of Molecular Biology, The Scripps Research Institute, La Jolla, California 92037.* [⊥]*Present address: A. N. Belozersky Institute of Physico-Chemical Biology, Moscow State University, Moscow 119899, Russia.*

Received May 12, 2010; Revised Manuscript Received July 14, 2010

ABSTRACT: Cytochrome ba_3 from *Thermus thermophilus* is a member of the family of B-type heme-copper oxidases, which have a low degree of sequence homology to the well-studied mitochondrial-like A-type enzymes. Recently, it was suggested that the ba_3 oxidase has only one pathway for the delivery of protons to the active site and that this pathway is spatially analogous to the K-pathway in the A-type oxidases [Chang, H.-Y., et al. (2009) *Proc. Natl. Acad. Sci. U.S.A. 106*, 16169−16173]. This suggested pathway includes two threonines at positions 312 and 315. In this study, we investigated the time-resolved reaction between fully reduced cytochrome ba_3 and O_2 in variants where Thr-312 and Thr-315 were modified. While in the A-type oxidases this reaction is essentially unchanged in variants with the K-pathway modified, in the Thr-312 → Ser variant in the ba_3 oxidase both reactions associated with proton uptake from solution, the $P_R \rightarrow F$ and $F \rightarrow O$ transitions, were slowed compared to those of wild-type ba_3. The observed time constants were slowed ∼3-fold (for $P_R \rightarrow F$, from 60 to ∼170 μs in the wild type) and ∼30-fold (for $F \rightarrow O$, from 1.1 to ∼40 ms). In the Thr-315 → Val variant, the $F \rightarrow O$ transition was ∼5-fold slower (5 ms) than for the wild-type oxidase, whereas the $P_R \rightarrow F$ transition displayed an essentially unchanged time constant. However, the uptake of protons from solution was a factor of 2 slower and decoupled from the optical $P_R \rightarrow F$ transition. Our results thus show that proton uptake is significantly and specifically inhibited in the two variants, strongly supporting the suggested involvement of T312 and T315 in the transfer of protons to the active site during O_2 reduction in the ba_3 oxidase.

The ba_3 cytochrome *c* oxidase (C*c*O)[1] from *Thermus thermophilus* is an integral membrane protein expressed at high temperatures and low oxygen concentrations. The ba_3 C*c*O is a member of the heme-copper oxidase (HCuO) superfamily, which consists of terminal oxidases that catalyze reduction of oxygen to water ($4e^- + 4H^+ + O_2 \rightarrow 2H_2O$) in a sequential mode; i.e., the reaction includes a number of reaction intermediates. The reaction is exergonic, and a fraction of its free energy is conserved in the form of a transmembrane electrochemical proton gradient. Energy conservation by terminal oxidases involves two different types of vectorial charge transfers: (i) a transfer of electrons and protons from opposite sides of the membrane [protons from the negative (in) N-side and electrons from the positive (out) P-side] to the catalytic site, where the oxygen chemistry occurs (eq 1a), buried in the membrane, and (ii) transfer of protons all across the membrane coupled to the redox reaction (proton pumping) (eq 1ab). The observed proton pumping stoichiometry (*n* in eq 1b) varies between different members of the HCuO superfamily; in the ba_3 C*c*O, ∼0.5 H^+/e^- is pumped (*1*), compared to ∼1 H^+/e^- for the aa_3-type oxidases.

$$O_2 + 4e^-_{out} + 4H^+_{in} \rightarrow 2H_2O \quad (1a)$$

$$nH^+_{in} \rightarrow nH^+_{out} \quad (1b)$$

According to the classification by Pereira et al., the *T. thermophilus* ba_3 C*c*O belongs to the B-type oxidases that display a low level of sequence identity to HCuO members of type A, such as the aa_3 C*c*Os found in mitochondria, *Rhodobacter sphaeroides*, or *Paracoccus denitrificans* (*2*). Like A-type HCuOs, the ba_3 C*c*O holds four redox-active sites, three of which are located in subunit I and include a low-spin heme *b* and a binuclear catalytic center consisting of a high-spin heme a_{s3} [with the farnesyl side chain replaced with a geranylgeranyl side chain (*3*)] and Cu_B. The fourth site is the dinuclear Cu_A center, located in subunit II, which acts as the primary electron acceptor from soluble cytochrome (cyt.) c^{552}. Amino acid residues, which serve as haem and Cu ligands, are conserved within the whole HCuO superfamily.

Like all other HCuOs, cytochrome ba_3 requires specialized proton-conducting pathways for the delivery of protons from the N-side of the membrane through the hydrophobic barrier to

[†]These studies were supported by grants from the Swedish Research Council (to P.B. and P.Ä.), by grant HL 16101 from the National Institutes of Health (to R.B.G.) and by the USPHS grant GM35342 (to J.A.F.). P.Ä. is a Royal Swedish Academy of Sciences Research Fellow supported by a grant from the Knut and Alice Wallenberg Foundation.

*To whom correspondence should be addressed. Telephone: +46-8-164183. Fax: +46-8-153679. E-mail: piaa@dbb.su.se.

[1]Abbreviations: DDM, *n*-dodecyl β-D-maltoside; F, ferryl intermediate; *k*, rate constant; PMS, phenazine methosulfate; P_R, peroxy intermediate; TMPD, *N*,*N*,*N*′,*N*′-tetramethyl-*p*-phenylenediamine; τ, time constant; WT, wild type; C*c*O, cytochrome *c* oxidase; HCuO, heme-copper oxidase. Unless otherwise noted, the numbering of amino acid residues refers to subunit I in the *T. thermophilus* ba_3 oxidase.

Published on Web 07/14/2010

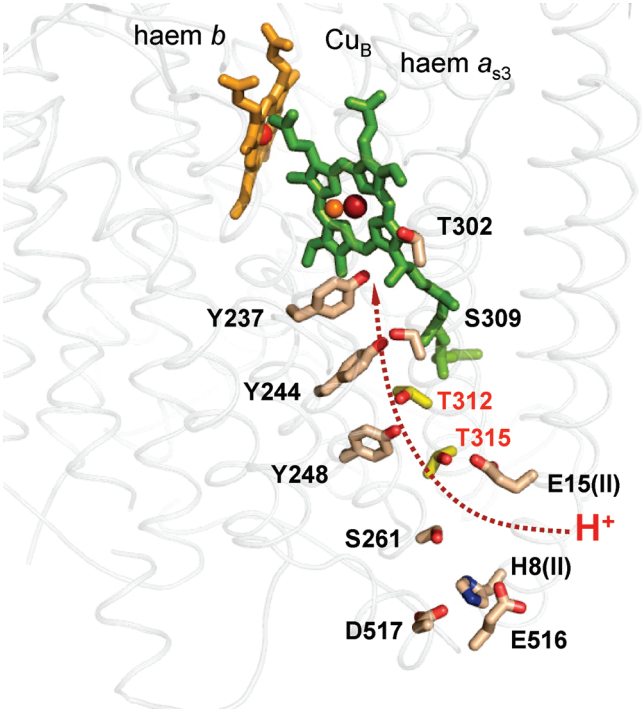

FIGURE 1: Overview of the suggested proton-conducting K-pathway in ba_3 C*c*O from *T. thermophilus* (Protein Data Bank entry 1EHK) (*3*, *8*). Helices and loops are shown as a light gray cartoon. Heme a_{s3} is colored green; heme *b* is colored light orange. Iron atoms of the hemes and copper of Cu_B are colored dark red and orange, respectively. Side chain atoms of the subunit I residues belonging to the proton-conducting pathway are shown as sticks. The residues that were modified in this work are labeled in scarlet. Water molecules of the pathway are not shown.

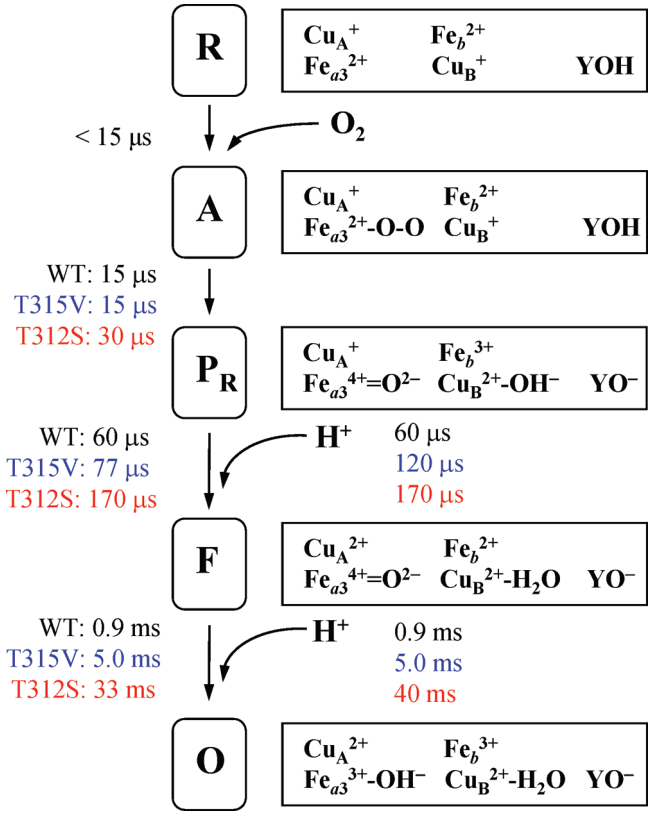

FIGURE 2: Reaction scheme illustrating the oxidative part of the reaction cycle of the ba_3 C*c*O, modified from ref *10*. The suggested structures of the intermediates are shown in rectangles to the right (Cu_A, copper A; Fe_b, iron ion of heme *b*; Cu_B, copper B; Fe_{a3}, iron ion of heme a_{s3}; Y, Tyr-237, the suggested proton donor in the active site). Time constants for the optical transitions in WT and the T312S and T315V variants are shown at the left, and the rate constants for proton uptake are shown to the right. Note that the R → A transition is not resolved in our measurements (but see ref *9*).

the binuclear catalytic center located approximately halfway through the membrane dielectric.

In a mitochondrial-like HCuO [the A1 type (*2*)], there are two proton-transfer pathways connecting the cytoplasmic compartment with the active site, called the D- and K-pathways, consisting of protonatable residues and water molecules (for a review of the general architecture of proton-transfer pathways, see ref *4*). The D-pathway is used for both substrate (used in water formation) and pumped protons during the oxidative part of the catalytic cycle, whereas the K-pathway is used for proton uptake during the reductive part (see, e.g., refs *5* and *6*). The D-pathway is named after an important aspartate (Asp-132, *R. sphaeroides* aa_3 numbering) located at the pathway entrance at the cytoplasmic surface, and the K-pathway is named after an essential lysine (Lys-362 in *R. sphaeroides* aa_3) in the middle of the pathway.

The three-dimensional structure of ba_3 C*c*O from *T. thermophilus* was determined, and originally, three putative proton-conducting channels, leading from the cytoplasmic surface to the catalytic site, were proposed (*3*). One of them has a location in space equivalent to that of the K-pathway in A-type HCuOs. The other suggested proton pathway overlaps in part with the D-pathway in A-type HCuOs and leads from the protein surface (Glu-17) to an internal cavity ~13 Å from the catalytic site. Protons may be transferred to the catalytic site either directly from this cavity or via residues (Thr-81, Thr-394, and Ser-391) that are shared with the third suggested proton pathway called the Q-pathway. This putative pathway starts at a different surface Glu (Glu-254) and leads to the junction with the D-pathway.

T. thermophilus ba_3 C*c*O has been cloned, enabling site-directed mutagenesis (*7*), which was used in a recent study in combination with sequence homology searches to suggest that B-type HCuOs use only one proton-conducting pathway (*8*). This pathway is the one equivalent to the K-pathway in the A-type oxidases, although it consists of other amino acids. The pathway (Figure 1) is built up mostly by residues in subunit I and leads to the conserved Tyr-237, which is covalently bound to the Cu_B ligand His-233. This pathway may start at the N-side of the membrane with Glu-516, Asp-517, and Ser-261 together with His-8(II) and Glu-15(II), where the latter two come from subunit II. Two of the residues of the K-pathway in *R. sphaeroides* aa_3 (Thr-359 and Lys-362) are replaced in ba_3 with Ser-309 and Thr-312, respectively. Other residues in the ba_3 pathway include Thr-315, Tyr-244, and Tyr-248 and two structural water molecules.

The reaction of fully reduced ba_3 C*c*O with oxygen was recently independently studied with time-resolved approaches by two groups (*9*, *10*). The basic reaction sequence of the oxidative part of the catalytic cycle was shown to be similar to that of the aa_3-type oxidase (Figure 2). Initially, reduced heme a_{s3} binds oxygen with formation of intermediate A ($k \sim 1.7 \times 10^8$ M^{-1} s^{-1}) (*9*). Next, three electrons are taken from the binuclear center and one is taken from the heme *b* to break the O−O bond, and an oxo−ferryl state (termed P_R) is formed at heme a_{s3} ($k \sim 6.8 \times 10^4$ s^{-1}). In the next step, a proton is taken from the solution to the binuclear center forming intermediate F and the electron on Cu_A re-equilibrates with heme *b* ($k \sim 1.7 \times 10^4$ s^{-1}). Finally, the fully oxidized state is formed in a process concomitant with the uptake of the second proton from the solution ($k \sim 1.1 \times 10^3$ s^{-1}).

In this study, we investigated the reaction between fully reduced ba_3 and O_2 in ba_3 C*c*O variants where Thr-312 and Thr-315 in the suggested proton pathway were replaced with Ser and Val, respectively. These mutations slowed enzyme turnover ~10-fold.

In the T312S variant, both transitions associated with the uptake of protons from solution, the $P_R \rightarrow F$ and $F \rightarrow O$ transitions, were slowed compared to that of wild-type ba_3 C*c*O and occurred simultaneously with the uptake of protons from solution. Also, in the T315V variant, the $F \rightarrow O$ transition was significantly slowed and coupled to proton uptake. However, the $P_R \rightarrow F$ transition occurred with an essentially unchanged rate constant, while the uptake of protons from solution was slowed by a factor of 2; i.e., it followed in time after the $P_R \rightarrow F$ transition. The reductive part of the catalytic cycle in ba_3 C*c*O was investigated using the stopped-flow technique. Neither of these mutations had any effect on the reduction of heme *b* or a_{s3}.

In other words, our results show that proton uptake during the oxidative phase of the reaction is significantly and specifically inhibited in the two variants, which supports the suggested involvement of T312 and T315 in the transfer of protons to the active site.

MATERIALS AND METHODS

Bacterial Growth and Protein Purification. *T. thermophilus* HB8 strain YC_1001 (including the deletion of the *cba* gene and a plasmid with the ba_3 gene with a hepta-His tag added at the N-terminus of subunit I) was used as a source of wild-type (WT) and variant cytochrome ba_3. Construction of the site-directed mutant ba_3 forms was described previously (*7*, *8*).

Cultivation of *T. thermophilus* HB8 and purification of the recombinant ba_3 C*c*O were performed essentially as described in ref *7*. Small aliquots of a concentrated solution of purified ba_3 C*c*O (60−80 μM) in 10 mM Hepes (pH 8.0) and 0.05% dodecyl β-D-maltoside (DDM) were kept at 4 °C or flash-frozen in liquid nitrogen; in the latter case, quick thawing was used to keep the enzyme intact. We observed no significant differences between the His-tagged WT ba_3 and the untagged enzyme studied previously (*10*).

Cytochrome c_{552} from *T. thermophilus* was purified as described in ref *11*.

Steady-State Activity. Steady-state activity was monitored by recording oxygen consumption with Clark-type electrodes (Hansatech Oxytherm) at 23 °C (295 K). The starting solution contained 100 mM Hepes (pH 7.5), 0.05% DDM, 6 mM ascorbate, 0.5 mM *N*′,*N*′,*N*′-tetramethyl-*p*-phenylenediamine (TMPD), and 5 μM cytochrome c_{552}. The signal was allowed to stabilize before the reaction was started by the addition of 5 nM ba_3 C*c*O.

Sample Preparation for Flow-Flash Measurements. The cytochrome ba_3 samples were prepared as previously described (*10*). Briefly, samples containing cytochrome ba_3 in 100 mM Hepes-NaOH (pH 7.5), 0.05% DDM, and 5 μM phenazine methosulfate (PMS) were made anaerobic on a vacuum line, and air was exchanged for nitrogen. The enzyme was completely reduced (four electrons per ba_3 C*c*O) by the addition of 2−3 mM sodium ascorbate and incubation from 1 h (at room temperature) to overnight (4 °C). Then, nitrogen was exchanged for carbon monoxide and the mixture incubated for ~1−2 h at room temperature. Prolonged incubation was avoided because of a noticeable decrease in heme *b* absorbance (see the Supporting Information).

Before the fully reduced CO-bound ba_3 oxidase was transferred to the flow-flash syringe, CO recombination after flash photolysis was assessed as a probe of the integrity of the binuclear site. The setup for CO flash photolysis was described in ref *12*.

Flow-Flash Experiments. Flow-flash experiments were performed using a locally modified stopped-flow apparatus (Applied Photophysics, DX-17MV) as described in ref *12*. The enzyme solution was mixed with an oxygen-saturated solution (~1.2 mM oxygen) at a ratio of 1:5, and the reaction of the enzyme with oxygen was initiated by flash photolysis (10 ns, 200 mJ, 532 nm, Nd:YAG laser from Quantel) of the enzyme−CO complex 30 ms after mixing. The short (30 ms) mixing time was used to minimize thermal dissociation of CO which has been shown to occur ~30-fold faster in ba_3 C*c*O than in aa_3-type HCuOs (*13*). Kinetics were monitored at different wavelengths (see the figures) and in two channels simultaneously so that traces were recorded on two different time scales after the flash. The traces were fit to a sum of kinetic components.

Kinetic amplitudes were normalized to 1 μM reactive enzyme based on the CO step at 445 nm using an ε of 67 mM^{-1} cm^{-1}.

Proton Uptake Measurements. Proton uptake during oxidation of the fully reduced enzyme by oxygen was assessed as described previously (*10*). Briefly, the pH indicator dye cresol red (pK_a = 8.3) was used because it has an absorbance maximum at 580 nm (deprotonated) where the contribution of the heme *b* absorbance is significantly decreased. The sample buffer was exchanged for a buffer-free solution [100 mM KCl and 0.05% DDM (pH 8.0−8.2)] using gel filtration on a prepacked Sephadex G-25 column (PD-10, GE Healthcare). Traces were also obtained in the presence of buffer [100 mM Hepes (pH 8.0)], and these traces were subtracted from those obtained in the buffer-free solution to exclude possible contributions from oxidation of the hemes or reaction intermediates. To determine the amount of protons taken up during the oxidation of ba_3, the exhaust from the stopped-flow apparatus was collected and the ΔA^{580} per micromolar H^+ determined as described previously (*10*).

Measurement of the Reduction Rate of the Hemes. Reduction of the hemes was monitored using a stopped-flow apparatus equipped with a diode array accessory (Applied Photophysics, SX-20 series). A solution of ~5 μM ba_3 in the oxidized form (as purified) in 100 mM Hepes-NaOH (pH 7.5), 0.1% Triton X-100, and 0.05% DDM was mixed with an equal volume of the same buffer (without Triton X-100) containing 30 mM dithionite as a reductant and either 10 mM TMPD or 10 μM cytochrome c_{552} as a mediator. The diode array enabled us to monitor absorbance changes at multiple wavelengths simultaneously. For data evaluation, we subtracted a reference trace from the trace at the absorbance maximum of the individual hemes to minimize artifacts from baseline drift or periodical noise. The reduction reactions of hemes *b* and a_{s3} (see below for extinction coefficients) were monitored at 562.1 nm (with a reference wavelength of 575 nm) and 611.4 nm (with a reference wavelength of 631.1 or 650.8 nm), respectively. Approximately seven traces were averaged. The rate constants were obtained by fitting the traces to a sum of kinetic components. The amount of heme reduced during the course of the reaction was estimated from the reduced minus oxidized difference spectrum (see below), where the spectra obtained after 1 ms and ~5 min represent those of the oxidized and reduced species, respectively.

Determination of the Heme Concentrations. The heme *b* concentration was determined from a heme *b* reduced absolute

spectrum with an $\varepsilon(560-590)$ of 26 mM^{-1} cm^{-1} (*7*) or from a heme *b* reduced minus oxidized spectrum with an $\varepsilon(560-658)$ of 21 mM^{-1} cm^{-1} (*14*). Ferro-heme a_{s3} was quantified using an $\varepsilon(613-658)$ of 6.3 mM^{-1} cm^{-1} in the reduced minus oxidized spectrum (*14*). The CO complex was quantified using an $\varepsilon(593-613)$ of 8.0 mM^{-1} cm^{-1} from the CO-reduced minus reduced spectrum (*14*).

RESULTS

Steady-State Activity. Turnover numbers measured with ascorbate, cytochrome c_{552}, and TMPD (see Materials and Methods) at pH 7.5 in the different ba_3 variants were as follows: ~200 electrons/s the wild type, ~15 electrons/s for T312S, and ~20 electrons/s for T315V. These values are in agreement with previously published data (*8*).

Optical Spectra and CO Recombination. A sample for a flow-flash experiment contains the reduced enzyme where heme a_{s3} is ligated with CO. Upon sample preparation (see Materials and Methods), we noted some spectral differences in the T312S and T315V ba_3 variants compared to WT (described in the Supporting Information). These changes are, however, not expected to influence the interpretation of our kinetic data.

CO recombination with the a_{s3} heme of the fully reduced ba_3 was studied as a probe of the integrity of the active site, and the observed rate constants were as follows: 5.1 s^{-1} for the wild type, 4.6 s^{-1} for T312S, and 3.5 s^{-1} for T315V; i.e., the rate constants were approximately the same for the different forms of the ba_3 C*c*O.

Rapid Absorbance Changes during the Reaction between Fully Reduced ba_3 Variants and O_2. When the reduced CO-bound ba_3 is mixed with an oxygenated solution, no reaction can proceed before CO is dissociated from the catalytic site. A short laser flash, applied shortly after mixing, releases CO and allows binding of O_2 and its sequential reduction to water. In the flow-flash apparatus, we detect the formation and decay of reaction intermediates using absorption spectroscopy.

We previously characterized the reaction between fully reduced wild-type ba_3 from *T. thermophilus* and O_2 (*10*) (see also ref *9*). Briefly, after the unresolved dissociation of CO from heme a_{s3}, the first phase we observe is ascribed to P_R formation at a *k* of 6.8×10^4 s^{-1} ($\tau \sim 15$ μs). The second phase, with a rate constant of 1.7×10^4 s^{-1} ($\tau \sim 60$ μs), is attributed to formation of the F[2] intermediate and re-reduction of heme *b*, concomitant with the uptake of protons from solution (see below).

Formation of F is followed by a (major) phase with a rate constant of 1100 s^{-1} ($\tau \sim 0.9$ ms), associated with the transfer of the last electron from heme *b* and formation of the fully oxidized enzyme. Formation of O also has a small (< 10% at all observed wavelengths) contribution from a phase with a rate constant of ~200 s^{-1} ($\tau \sim 5$ ms). Figure 3 shows the observed absorbance changes at 445 nm (reporting mainly on heme a_{s3}), 430 nm (mainly heme *b*), 560 nm (heme *b*), and 610 nm (heme a_{s3}).

The T312S and T315V variants exhibited kinetic characteristics different from those of WT C*c*O; the data are summarized in Table 1 and described below.

(*i*) *T312S*. Formation of the P_R state was slowed ~2-fold in T312S to a rate of $\sim 3.3 \times 10^4$ s^{-1} [$\tau \sim 30$ μs (see Figure 3)]. The second phase, attributed to the $P_R \rightarrow F$ transition, was slowed more significantly (~3-fold) to a *k* of ~6000 s^{-1} ($\tau \sim 170$ μs) and coupled to the uptake of protons from solution (see below).

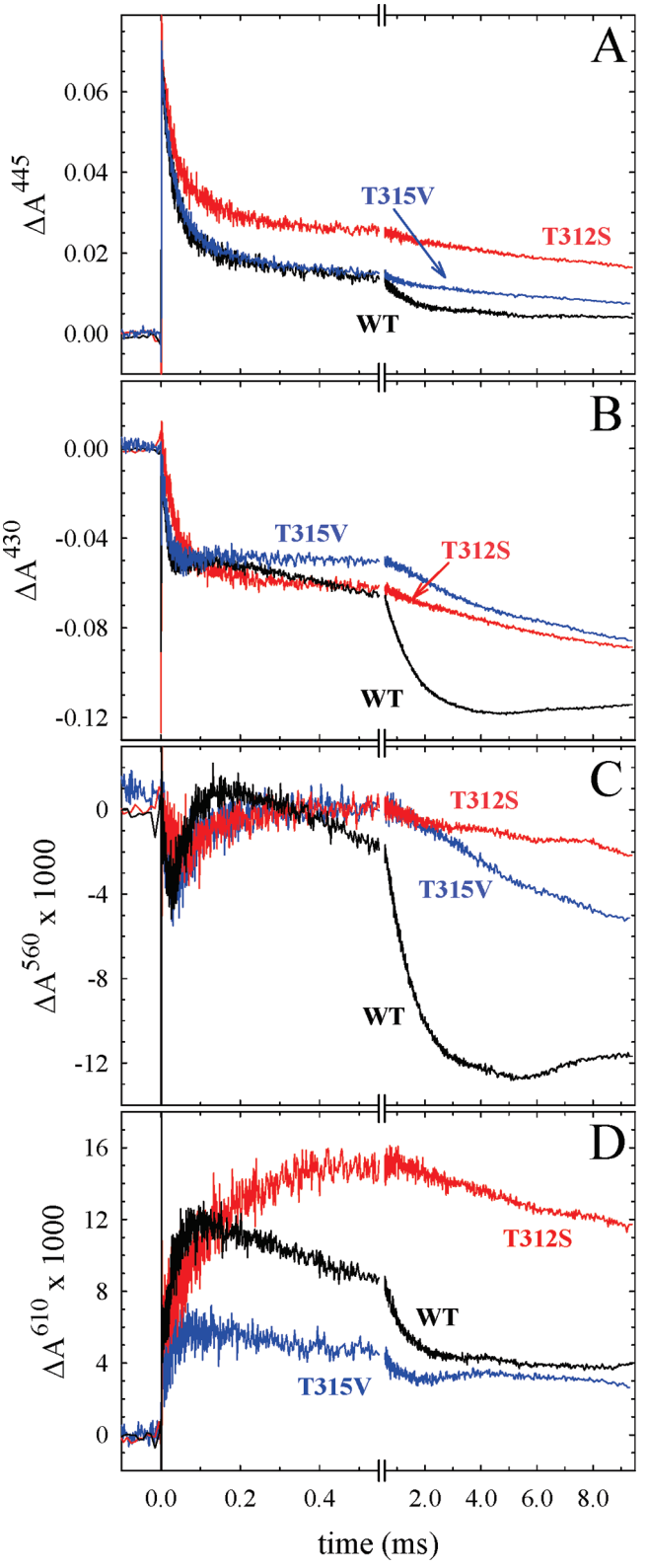

FIGURE 3: Absorbance changes associated with reaction of the fully reduced ba_3 C*c*O with oxygen. Traces for WT, T312S, and T315V are colored black, red, and blue, respectively. The absorbance changes were monitored at 445 (A), 430 (B), 560 (C), and 610 nm (D). Experimental conditions: 100 mM Hepes-KOH (pH 7.5), 0.05% DDM, 295 K. Amplitudes are normalized to 1 μM reacting ba_3. The CO ligand was dissociated by a laser flash at time zero.

[2]Note that in ba_3 C*c*O, formation of F is in itself not associated with any detectable absorbance change (*9*), as occurs in aa_3, where the peak shifts from 607 to 580 nm (*15*).

Table 1: Rate Constants of the Transitions Observed in the Flow-Flash Experiments

	rate constant (s^{-1})		
	P_R formation	P_R to F transition	F to O transition
WT	6.8×10^4	1.7×10^{4a}	1.1×10^3
T312S	3.3×10^4	6.0×10^{3a}	30
T315V	6.8×10^4	1.3×10^{4b}	200

[a]The P_R to F transition was monitored indirectly via transient re-reduction of heme *b* and proton uptake. [b]The P_R to F transition was monitored via transient re-reduction of heme *b*; proton uptake occurred at a *k* of $\sim 8.5 \times 10^3$ s^{-1}.

The final step, formation of the oxidized enzyme, was slowed ~30-fold and occurred at ~30 s^{-1} ($\tau \sim 33$ ms) in T312S.[3]

The absorbance maximum for reduced heme *b* in the α-region is at 560 nm. According to the obtained amplitude of the $P_R \rightarrow F$ transition in T312S, a smaller fraction of heme *b* was reduced during F formation (Figure 3C) in this variant compared to the WT C*c*O. The redox state of heme *b* is monitored also at 430 nm, where the initial decrease in absorbance is dominated by oxidation of heme *b* during P_R formation. At this wavelength, the subsequent increase in absorbance associated with transient reduction of heme *b* during the $P_R \rightarrow F$ transition is less clearly seen in the T312S ba_3 variant than in the WT enzyme, consistent with a smaller fraction reduced heme *b*.

(*ii*) *T315V*. The rate constant for P_R formation was unchanged in the T315V mutant C*c*O, whereas the $P_R \rightarrow F$ transition ($k \sim 1.7 \times 10^4$ s^{-1} in WT) was slightly slowed to $\sim 1.3 \times 10^4$ s^{-1} and uncoupled from the uptake of protons from solution, which was ~1.5-fold slower [~8000 s^{-1} (see below)]. The final $F \rightarrow O$ transition occurred with a rate constant of ~200 s^{-1} ($\tau \sim 5$ ms).

Rapid Proton Uptake during Oxidation of the Fully Reduced ba_3. Proton uptake associated with oxidation of the fully reduced ba_3 C*c*O was monitored with the pH-sensitive dye cresol red (Figure 4) at pH ~8.0 as described in ref *10*. The WT ba_3 C*c*O displays two major phases of proton uptake with rate constants of $\sim 1.7 \times 10^4$ and ~1100 s^{-1} and approximately equal contributions, corresponding to formation of F and O intermediates, respectively. The net total proton uptake stoichiometry was ~1.5 H^+/ba_3.

In the T312S variant, two phases of proton uptake were observed with rate constants of ~6000 and ~25 s^{-1}, corresponding to the rate constants observed for the $P_R \rightarrow F$ and $F \rightarrow O$ transitions, respectively. The amplitude ratio of the fast phase ($P_R \rightarrow F$) to the slow phase ($F \rightarrow O$) was ~1:1.

In the T315V variant, the first phase of proton uptake was observed with a rate constant of ~8500 s^{-1}, which was ~1.5-fold slower than the corresponding $P_R \rightarrow F$ transition (see Discussion below). The second phase had a rate constant of 200 s^{-1}, i.e., occurred concomitantly with the $F \rightarrow O$ transition. The amplitude ratio was ~1:1.

Both the T312S and T315V variants exhibited total proton uptake stoichiometry similar to that of the WT ba_3 C*c*O (Figure 4).

Reduction of Oxidized ba_3 Variants. Reduction of ba_3 C*c*O was demonstrated to be much slower than oxidation (*8*) and could be studied using a stopped-flow apparatus. In this study, we used two systems of reductants: dithionite with either TMPD (as in ref *8*) or with cytochrome c_{552} (the native reductant). The use of dithionite as the ultimate electron donor enabled mixing with an aerobic enzyme sample, since rapid scavenging of oxygen occurred during the mixing time of the instrument. The results showed that neither of the investigated mutations had a significant impact on the reduction rates (Table 2).

[3]In one T312S preparation, there was an additional phase that we have not assigned to any transition, with a *k* of ~250 s^{-1}, observed at 445 nm, contributing < 20% to the total absorbance shift.

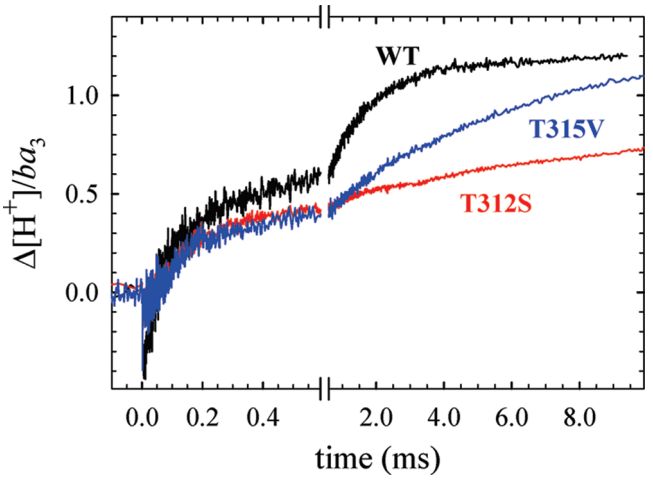

FIGURE 4: Proton uptake upon reaction of the fully reduced WT, T312S, and T315V ba_3 C*c*O with oxygen. Each trace is the difference between the averaged trace obtained without buffer and that in the presence of buffer (see Materials and Methods). The trace for the WT enzyme is from ref *10*. The amplitudes are normalized to 1 μM reacting enzyme. $\Delta H^+/ba_3$ values were determined as described in Materials and Methods. Experimental conditions: 100 mM KCl, 0.05% DDM, pH 8.0−8.2, 40 μM cresol red. Other conditions were as described in the legend of Figure 3.

Table 2: Reduction of Cytochrome ba_3 upon Being Mixed with the Indicated Reductants and Mediators at 295 K[a]

	rate in 15 mM dithionite and 5 mM TMPD (s^{-1})		rate in 15 mM dithionite and 5 μM cytochrome c_{552} (s^{-1})	
	heme *b*	heme a_{s3}	heme *b*	heme a_{s3}
WT	31	13	51	12
T312S	33	11	48	10
T315V	28	15	53	10

[a]For reaction conditions and details, see Materials and Methods.

DISCUSSION

When the three-dimensional structure of ba_3 C*c*O from *T. thermophilus* was determined (*3*; see also ref *16*), three putative proton-conducting pathways (called D, Q, and K) were proposed (*3*). Sequence analysis in combination with site-directed mutagenesis indicated that only one of these pathways is functionally important for proton delivery (*8*), and it was suggested that the B-type oxidases use only one proton delivery pathway for both substrate (used for water formation) and pumped protons. This is in contrast to the A-type HCuOs which use two different pathways (D and K) for proton transfer during different partial steps in the catalytic cycle: the D-pathway for protons (6−7) taken up during the oxidative phase (both chemical and pumped) and the K-pathway for protons (1−2) taken up during reduction (see, e.g., refs *5* and *17*).

In cytochrome ba_3, the suggested proton-transfer pathway has a spatial location similar to that of the K-pathway in the aa_3-type oxidases, although it consists of different amino acid residues. The key residue of the K-pathway in *R. sphaeroides* aa_3 (Lys-362) is replaced in the ba_3 C*c*O by Thr-312. Thr-315 sits slightly "below" (toward the cytoplasmic side) Thr-312 in the pathway (see Figure 1). Introduction of a T312S or T315V mutation resulted in a decrease in the ba_3 turnover rate from ~200 to 15−20 e^-/s (ref *8* and this study). Additionally, introduction of a valine at position 315 (but not a serine at position 312) deprived the ba_3 of proton pumping activity (*8*).

Application of the flow-flash technique allowed us to pinpoint which (if any) partial steps of the oxidative half (reaction of the reduced cytochrome ba_3 with O_2) of the reaction cycle were affected by these mutations. A sequential scheme of the reaction of the four-electron reduced cytochrome ba_3 with oxygen is shown in Figure 2. Two reaction steps involve the uptake of protons from the solution, the $P_R \rightarrow F$ and $F \rightarrow O$ transitions. Our results show that in both the T312S and T315V ba_3 variants, these transitions are slowed, which is in contrast to the situation in the aa_3-type C*c*Os, where alterations of residues in the K-pathway have no significant effect on these transitions (see, e.g., ref *18*). Our results, discussed in more detail below, thus support the involvement of the T312 and T315 residues in the delivery of protons to the active site.

T312S. In T312S ba_3, the $P_R \rightarrow F$ transition rate constant decreased from $\sim 1.7 \times 10^4$ s^{-1} (in WT) to ~6000 s^{-1}, an ~3-fold retardation. The rate constant for the $F \rightarrow O$ transition was slowed a factor of ~30, from ~1100 to ~30 s^{-1}.

Surprisingly, we observed an ~2-fold retardation (rate constant changed from $\approx 6.8 \times 10^4$ to $\approx 3.3 \times 10^4$ s^{-1}) also upon formation of the P_R state in the T312S mutant, while this step does not involve any external proton in aa_3-type oxidases or cytochrome ba_3 (ref *10* and this study). However, in aa_3 C*c*O, the formation of P_R has been shown to involve internal proton transfer (*19*, *20*) from the active-site Tyr to break the O−O bond (*21*, *22*). Furthermore, in *R. sphaeroides* aa_3 C*c*O, formation of P_R was slowed in variants where residues in the K-pathway were modified, and it was suggested that the positively charged K362 (which is spatially analogous to T312 in ba_3) changes conformation during formation of P_R to charge-compensate for the additional negative charge in the active site (*12*). Although Thr-312 in ba_3 cannot be positively charged, the same principle of using alterations in the pathway to accommodate the change in charge at the active site might still apply and explain the small slowing of the formation of P_R in the T312S variant.

The "central" role of T312 in the pathway is also manifested in the substantial effects on the rates of proton transfer even though a change from threonine to serine is relatively modest.

T315V. In the oxidative half of the catalytic cycle, the T315V mutation affected mostly the $F \rightarrow O$ transition, for which the rate constant was ~6-fold slower (~200 s^{-1}) than in the WT ba_3 (~1100 s^{-1}). The $P_R \rightarrow F$ transition occurred nearly as fast as in the WT enzyme (~1.3×10^4 s^{-1} compared to ~1.7×10^4 s^{-1}). However, the uptake of protons from solution was slower ($k \sim 8500$ s^{-1}) than the optical transition, which is in contrast to the WT and T312S variants where these processes had the same rate constants. This observation can be explained by an internal proton transfer occurring with a k of ~1.3×10^4 s^{-1}, enabling the $P_R \rightarrow F$ transition to take place, although the uptake of protons from solution is indeed slowed. This scenario is similar to that in the D132N variant of the aa_3 C*c*O in *R. sphaeroides* (*23*), where the uptake of protons from solution is significantly slower than the $P_R \rightarrow F$ transition at the catalytic site. It should also be noted that in the model for the $P_R \rightarrow F$ transition in aa_3, the internal proton transfer is the rate-limiting step at a k of ~10^4 s^{-1}, and the uptake of protons from solution occurs with a k of $\gg 10^4$ s^{-1} (*23*). Translated to the scenario in the ba_3 oxidase, the observed retardation of proton uptake in the T315V mutant C*c*O to a k of ~8500 s^{-1} is then due to slowed proton transfer from $\gg 1.7 \times 10^4$ s^{-1} such that the actual retardation is much larger than the observed factor of ~2.

Because in T315V, the valine at position 315 is incapable of proton transfer, it can presumably be bypassed via a different residue indicating that Thr-315 is not as central to the functioning of the pathway as Thr-312.

It should, however, be noted that the T315V mutation leads to a decoupling of the proton pump, in contrast to the T312S mutant which retains pumping (*8*). Because in our flow-flash measurements, the observed transitions in T312S ba_3 are more significantly slowed than in T315V ba_3, this decoupling is not simply a result of slowing of the uptake of protons from the bulk solution. Instead, it is likely that the decoupling is due to changes in the timing of internal proton transfers in the T315V mutant C*c*O, which would determine the pumping stoichiometry. In this mutant, C*c*O proton uptake is decoupled from the optical $P_R \rightarrow F$ transition (which requires the transfer of protons to the catalytic site), which would lead to accumulation of an unprotonated form of an internal proton donor to the catalytic site.

We also note that in both the T312S and T315V variants, the $F \rightarrow O$ transition is more affected than the $P_R \rightarrow F$ transition, which is presumably linked to the observation that in ba_3 C*c*O, only the $F \rightarrow O$ transition (and not $P_R \rightarrow F$) is linked to the pumping of protons across the membrane (*9*). This is in contrast to the situation in aa_3 C*c*O, where both the $P_R \rightarrow F$ and $F \rightarrow O$ transitions are linked to proton pumping (see, e.g., ref *24*).

In the T312S and T315V ba_3 variants, the oxidative part of the catalytic cycle is affected, whereas the reductive part is largely unaffected (see Table 2). This is in contrast to the situation in the T312V and E15A (in SU-II) ba_3 variants which were shown to be inhibited in both the oxidative and reductive parts of the reaction cycle (*8*). These mutations resulted in such significant retardation of the catalytic cycle that it was possible to use stopped-flow for studying the oxidative phase. The observed retardation of both oxidative and reductive phases is different from the situation in aa_3-type oxidases, where mutations in the D-pathway affect mainly the oxidative phase and mutations in the K-pathway affect mainly the reductive phase (see, e.g., ref *5*). The retardation of both reduction and oxidation in the T312V and E15A ba_3 variants was thus seen as further evidence of the existence of only one proton pathway. However, even in the wild-type enzyme, the observed rate of reduction of heme a_{s3} is slow [~10−15 s^{-1} (see Results and ref *8*)]. This is possibly due to the use of the "as isolated" form of the ba_3 C*c*O, since the bovine C*c*O is known to reduce more slowly in the so-called "resting" state than in the so-called "pulsed" (recently oxidized; see ref *25* and references therein) form. It is thus possible that the serine at position 312 (T312S) or the bypass of the valine at position 315 (T315V) is sufficient for the delivery of protons during these slower reactions of the reductive part of the cycle, while each fails to fulfill this task during the fast reactions of the oxidative part. It is also possible that differences in the reduction rates between the wild type and T312S and T315V variants would be observed under conditions where reduction of heme a_{s3} is faster.

In conclusion, in this study we have focused on partial reaction steps during the catalytic cycle specifically linked to proton transfer, and our results show that altering K-pathway residues T312 and T315 in ba_3 oxidase from *T. thermophilus* inhibits proton transfer during the oxidative phase and support the identification of a proton pathway through T312 and T315.

ACKNOWLEDGMENT

Ying Chen (The Scripps Research Institute) is acknowledged for assistance in the introduction of mutations and the preparation of mutant proteins.

SUPPORTING INFORMATION AVAILABLE

Optical spectra of WT, T312S, and T315V ba_3. This material is available free of charge via the Internet at http://pubs.acs.org.

REFERENCES

1. Kannt, A., Soulimane, T., Buse, G., Becker, A., Bamberg, E., and Michel, H. (1998) Electrical current generation and proton pumping catalyzed by the ba_3-type cytochrome c oxidase from *Thermus thermophilus*. *FEBS Lett*. *434*, 17–22.
2. Pereira, M. M., Santana, M., and Teixeira, M. (2001) A novel scenario for the evolution of haem-copper oxygen reductases. *Biochim. Biophys. Acta 1505*, 185–208.
3. Soulimane, T., Buse, G., Bourenkov, G. P., Bartunik, H. D., Huber, R., and Than, M. E. (2000) Structure and mechanism of the aberrant ba_3-cytochrome c oxidase from *Thermus thermophilus*. *EMBO J. 19*, 1766–1776.
4. Wraight, C. A. (2006) Chance and design: Proton transfer in water, channels and bioenergetic proteins. *Biochim. Biophys. Acta 1757*, 886–912.
5. Brzezinski, P., and Ädelroth, P. (1998) Pathways of proton transfer in cytochrome c oxidase. *J. Bioenerg. Biomembr. 30*, 99–107.
6. Konstantinov, A. A., Siletsky, S., Mitchell, D., Kaulen, A., and Gennis, R. B. (1997) The roles of the two proton input channels in cytochrome c oxidase from *Rhodobacter sphaeroides* probed by the effects of site-directed mutations on time-resolved electrogenic intraprotein proton transfer. *Proc. Natl. Acad. Sci. U.S.A. 94*, 9085–9090.
7. Chen, Y., Hunsicker-Wang, L., Pacoma, R. L., Luna, E., and Fee, J. A. (2005) A homologous expression system for obtaining engineered cytochrome ba_3 from *Thermus thermophilus* HB8. *Protein Expression Purif. 40*, 299–318.
8. Chang, H. Y., Hemp, J., Chen, Y., Fee, J. A., and Gennis, R. B. (2009) The cytochrome ba_3 oxygen reductase from *Thermus thermophilus* uses a single input channel for proton delivery to the active site and for proton pumping. *Proc. Natl. Acad. Sci. U.S.A. 106*, 16169–16173.
9. Siletsky, S. A., Belevich, I., Jasaitis, A., Konstantinov, A. A., Wikström, M., Soulimane, T., and Verkhovsky, M. I. (2007) Time-resolved single-turnover of ba_3 oxidase from *Thermus thermophilus*. *Biochim. Biophys. Acta 1767*, 1383–1392.
10. Smirnova, I. A., Zaslavsky, D., Fee, J. A., Gennis, R. B., and Brzezinski, P. (2008) Electron and proton transfer in the ba_3 oxidase from *Thermus thermophilus*. *J. Bioenerg. Biomembr. 40*, 281–287.
11. Fee, J. A., Chen, Y., Todaro, T. R., Bren, K. L., Patel, K. M., Hill, M. G., Gomez-Moran, E., Loehr, T. M., Ai, J., Thöny-Meyer, L., Williams, P. A., Stura, E., Sridhar, V., and McRee, D. E. (2000) Integrity of *Thermus thermophilus* cytochrome c552 synthesized by *Escherichia coli* cells expressing the host-specific cytochrome c maturation genes, ccmABCDEFGH: Biochemical, spectral, and structural characterization of the recombinant protein. *Protein Sci. 9*, 2074–2084.
12. Brändén, M., Sigurdson, H., Namslauer, A., Gennis, R. B., Ädelroth, P., and Brzezinski, P. (2001) On the role of the K-proton transfer pathway in cytochrome c oxidase. *Proc. Natl. Acad. Sci. U.S.A. 98*, 5013–5018.
13. Giuffrè, A., Forte, E., Antonini, G., D'Itri, E., Brunori, M., Soulimane, T., and Buse, G. (1999) Kinetic properties of ba_3 oxidase from *Thermus thermophilus*: Effect of temperature. *Biochemistry 38*, 1057–1065.
14. Zimmermann, B. H., Nitsche, C. I., Fee, J. A., Rusnak, F., and Munck, E. (1988) Properties of a copper-containing cytochrome ba_3: A second terminal oxidase from the extreme thermophile *Thermus thermophilus*. *Proc. Natl. Acad. Sci. U.S.A. 85*, 5779–5783.
15. Morgan, J. E., Verkhovsky, M. I., and Wikström, M. (1996) Observation and assignment of peroxy and ferryl intermediates in the reduction of dioxygen to water by cytochrome c oxidase. *Biochemistry 35*, 12235–12240.
16. Liu, B., Chen, Y., Doukov, T., Soltis, S. M., Stout, C. D., and Fee, J. A. (2009) Combined microspectrophotometric and crystallographic examination of chemically reduced and X-ray radiation-reduced forms of cytochrome ba_3 oxidase from *Thermus thermophilus*: Structure of the reduced form of the enzyme. *Biochemistry 48*, 820–826.
17. Wikström, M., Jasaitis, A., Backgren, C., Puustinen, A., and Verkhovsky, M. I. (2000) The role of the D- and K-pathways of proton transfer in the function of the haem-copper oxidases. *Biochim. Biophys. Acta 1459*, 514–520.
18. Ädelroth, P., Gennis, R. B., and Brzezinski, P. (1998) Role of the pathway through K(I-362) in proton transfer in cytochrome *c* oxidase from *R. sphaeroides*. *Biochemistry 37*, 2470–2476.
19. Hallén, S., and Nilsson, T. (1992) Proton transfer during the reaction between fully reduced cytochrome c oxidase and dioxygen: pH and deuterium isotope effects. *Biochemistry 31*, 11853–11859.
20. Karpefors, M., Ädelroth, P., Namslauer, A., Zhen, Y., and Brzezinski, P. (2000) Formation of the "peroxy" intermediate in cytochrome c oxidase is associated with internal proton/hydrogen transfer. *Biochemistry 39*, 14664–14669.
21. Proshlyakov, D. A., Pressler, M. A., and Babcock, G. T. (1998) Dioxygen activation and bond cleavage by mixed-valence cytochrome c oxidase. *Proc. Natl. Acad. Sci. U.S.A. 95*, 8020–8025.
22. Gorbikova, E. A., Belevich, I., Wikström, M., and Verkhovsky, M. I. (2008) The proton donor for O−O bond scission by cytochrome c oxidase. *Proc. Natl. Acad. Sci. U.S.A. 105*, 10733–10737.
23. Smirnova, I. A., Ädelroth, P., Gennis, R. B., and Brzezinski, P. (1999) Aspartate-132 in cytochrome c oxidase from *Rhodobacter sphaeroides* is involved in a two-step proton transfer during oxo-ferryl formation. *Biochemistry 38*, 6826–6833.
24. Faxén, K., Gilderson, G., Ädelroth, P., and Brzezinski, P. (2005) A mechanistic principle for proton pumping by cytochrome c oxidase. *Nature 437*, 286–289.
25. Verkhovsky, M. I., Morgan, J. E., and Wikström, M. (1995) Control of electron delivery to the oxygen reduction site of cytochrome c oxidase: A role for protons. *Biochemistry 34*, 7483–7491.